Behavioural Brain Research 197 (2009) 103–108

Contents lists available at ScienceDirect

Behavioural Brain Research

journal homepage: www.elsevier.com/locate/bbr

Research report

Detection of PCC functional connectivity characteristics in resting-state fMRI in mild Alzheimer's disease

Hong-Ying Zhang[a], Shi-Jie Wang[b], Jiong Xing[c], Bin Liu[a], Zhan-Long Ma[a], Ming Yang[a], Zhi-Jun Zhang[d], Gao-Jun Teng[a,*]

[a] Department of Radiology, Zhong-Da Hospital, Southeast University, Nanjing 210009, China
[b] Lab of Imaging Science and Technology, Southeast University, Nanjing 210096, China
[c] Department of Radiology, Methodist Hospital at Houston, Weil Cornell Medical College, United States
[d] Department of Neurology, Zhong-Da Hospital, Southeast University, Nanjing 210009, China

ARTICLE INFO

Article history:
Received 26 February 2008
Received in revised form 1 August 2008
Accepted 6 August 2008
Available online 22 August 2008

Keywords:
Resting-state functional MRI
Alzheimer's disease
Posterior cingulated cortex
Functional connectivity
Neural networks

ABSTRACT

Resting-state networks dissociate in the early stage of Alzheimer's disease (AD). The posterior cingulate cortex (PCC) in AD brain is vulnerable to isolation from the rest of brain. However, it remains unclear how this functional connectivity is related to PCC changes. We employed resting-state functional MRI (fMRI) to examine brain regions with a functional connection to PCC in a mild AD group compared with matched control subjects. PCC connectivity was gathered by investigating synchronic low frequency fMRI signal fluctuations with a temporal correlation method. We found asymmetric PCC-left hippocampus, right dorsal–lateral prefrontal cortex and right thalamus connectivity disruption. In addition, some other regions such as the bilateral visual cortex, the infero-temporal cortex, the posterior orbital frontal cortex, the ventral medial prefrontal cortex and the precuneus showed decreased functional connectivity to the PCC. There were also some regions, primarily in the left frontal–parietal cortices, that showed increased connectivity. These regions included the medial prefrontal cortex, bilateral dorsal–lateral prefrontal cortex, the left basal ganglia and the left primary motor cortex. Impairments to memory, high vision-related functions and olfaction in AD can be explained by a disruption to the functional connection of resting-state networks. The results of increased connectivity may support the compensatory-recruitment hypothesis. Our findings suggest that the characteristics of resting-state functional connectivity could plausibly provide an early imaging biomarker for AD.

1. Introduction

The proposition that Alzheimer's disease (AD) is a kind of neuro-disconnection syndrome is supported by evidence from neuropathological, electrophysiological, and neuroimaging studies [1]. Neuro-disconnection within organized networks may play an important role. Although little is known about the disconnection of different brain regions in AD, neuronal dysfunction in AD brain should not simply be ascribed as a local disorder.

Two principal neuropathological markers of Alzheimer's disease, neurofibrillary tangles (NFT) and neuritic plaques (NP), impair neuronic structure and decrease its function. These pathologic changes in AD disrupt neuronal circuits or tracts between different brain regions, and may be indicated by decreased nicotinic receptor levels in the frontal and parietal cortex and the loss of axons in pathways of neocortex [2–4]. Recent findings in mouse models of AD show that axons are important sites of cellular pathology and larger neurons with long axons are impressionably affected [4]. Moreover, neuropathology research from postmortem examinations in AD patients have revealed that neocortical NFT densities hold a more significant correlationship with Clinical Dementia Rating (CDR) than NP densities [5,6].

Functional connectivity (FC), which may be defined as the correspondence over time between spatially distinct neurophysiological events without implying directionality, may be observed from the spontaneous activity of the resting brain [7]. Although functional magnetic resonance imaging (fMRI) is most often applied to identify areas of increased activity in relation to specific tasks, recent advances reveal that synchronous low frequency fluctuations (LFF) signals within blood oxygen level-dependent fMRI data can be useful for investigating the functional connections of brain cortices. Brain cortices are characterized by LFF frequencies less than 0.1 Hz, which are distinct from respiratory and cardiac effects, the main components of physiological noise, with a frequency spectrum

* Corresponding author. Tel.: +86 25 83272121; fax: +86 25 83311083.
E-mail address: gjteng@vip.sina.com (G.-J. Teng).

0166-4328/$ – see front matter © 2008 Elsevier B.V. All rights reserved.
doi:10.1016/j.bbr.2008.08.012

ranging from 0.1 to 0.5 Hz and 0.6 to 0.12 Hz, respectively [8]. The synchrony of LFF implies that within neural networks, the nodes function together. Biswal et al. [9] were the first to observe coherent low frequency fluctuations in resting state fMRIs in bilateral motor related brain regions. LFF is widely employed in many fMRI studies to explore networks involved in primary motor, primary sensor, auditory, visual, language [8–11], even connectivity during associative episodic memory processes [12]. However, only a few fMRI studies have been conducted to explore this topic which revealed abnormal FC changes in the resting state (default mode) fMRI in AD. For example, Li et al. [13] observed decreased LFF synchrony within the hippocampus in early AD; and He et al. [14] found a significant decrease in LFF regional coherence in regions of the posterior cingulate cortex and precuneus (PCC/PCu) in mild AD. Greicius et al. [15] showed with an independent component analysis method that in mild AD, FC is deficient between the PCC and left hippocampus or other regions within default network. Wang et al. [16] found, with a seeding approach, that connectivity between the seed of right hippocampus and a set of regions was disrupted in the early stage of AD, whereas the seed of left hippocampus showed increased connectivity with some other regions. Sorg et al. [17] revealed that selective resting state functional connectivity between the bilateral hippocampus and the PCC was absent at high risk stage cases of AD with mild cognitive impairment. However, from above the literature, it is not consistent whether the FC between the paired hippocampus and the PCC is affected symmetrically. Thus, it is necessary to further study the characteristics of FC within resting state networks.

In the current study, we utilized the PCC as the region of interest (ROI) to study its altered connections with other brain regions. PCC is commonly identified as a critical node in the traditional default-mode network. FMRI and PET studies of humans have demonstrated the default mode network involved with the PCC, linking regions of the bilateral MPFC, hippocampus, posterior thalamus, inferior parietal cortex (IPC), precuneus and inferior lateral temporal cortex (ITC) [18–20]. A number of studies suggest that the PCC plays an essential role in spatial orientation, self appraisal and internal monitoring as well as memory processing [18,19,21,22]. PCC is also one of the earliest marker regions to predict cognitive decline, its metabolism and regional blood flow can be used to evaluate whether an individual with mild cognitive impairment will soon develop AD [23,24]. This convenging evidence shows that the networks associated with the PCC in AD mechanisms deserve deeper investigation.

The temporal correlation method has been successfully applied in previous FC fMRI studies [11,16,19,25], in these studies the seed regions were defined by prior task-induced fMRIs or using manual drawings. Here we used a PCC template that was obtained from a public software to define the seed region [26,27]. We hypothesize that functional connectivity will dissociate within the default networks associated with the PCC in the early AD stage, and increased function connectivity will occur in sub-regions of the frontal–parietal cortices, as pathological examinations have demonstrated that impairments occur later in these brain lobes [28,29], and these lobes may be recruited to play a compensatory role in the earlier stage.

2. Materials and methods

2.1. Subjects

Patients with AD were recruited from the geropsychiatry clinic department at Nanjing Brain Hospital, and the geratology clinic department at Zhongda Hospital, Nanjing, China. Control subjects were recruited from local communities.

The subjects groups consisted of 18 patients with possible or probable AD at the early or mild stage, and 16 control subjects. All subjects were right-handed.

Table 1
Summary of subject demographic information

	NC	Mild AD	*p* value
n	16	16	
Age (years)	71.3 ± 4.9	71.6 ± 5.1	0.96
Education (years)	10 ± 4.9	9.6 ± 5.5	0.88
Sex (M/F)	7/9	6/10	0.91
MMSE	28.5 ± 1.1	22 ± 3.5	0.0001

NC = normal control; CDR = Clinical Dementia Rating; MMSE = mini mental state examination.
p values were obtained by *F*-test.

All patients met the Diagnostic and Statistical Manual of Mental Disorders, 4th Edition (DSM-IV) criteria for dementia, and the National Institute of Neurological and Communicative Disorders and Stroke/AD and Related Disorders Association (NINCDS-ADRDA) diagnostic criteria for possible or/and probable AD. The AD patients were diagnosed by at least two veteran geropsychiatric doctors. The patients' CDR scores ranged between 0.5 and 1, and their mini mental state examination (MMSE) scores fell within the range of 20–24. All AD patients who had been receiving cholinesterase inhibitor treatment stopped treatment 2 weeks prior to fMRI scanning. The remaining patients had never before taken these medications.

Control subjects were healthy volunteers of age and education degrees similar to the patients, have no memory impairment or cognitive disorders, and had no abnormal findings on their conventional brain MRI examination. Their MMSE scores ranged from 28 to 30 and CDR scores were all zero. Demographic characteristics and neuropsychological scores are shown in Table 1.

This study was approved by the Southeast University Ethics Committee. Prior to performing each fMRI, all subjects or their guardians gave informed consent to participate in the study.

2.2. Data acquisition

All subjects wore headphones and were instructed to lie in a supine position and imaged by a standard head coil of a 1.5T Philips Eclipse MR scanner in a dim scan room. Form padding was used to limit head movement. Structural images (the axial, sagittal T1WI, and axial T2 FLAIR sequences) were performed first. Then the resting-state fMRI was performed, where subjects were instructed to lie quietly still with their eyes closed and to clear their heads of all thoughts. Functional images were acquired by using a gradient echo-planar imaging (EPI) sequence (TR = 3000 ms, TE = 40 ms, flip angle = 90, slice thickness = 6 mm, slice gap = 0 mm, FOV = 240 mm, matrix = 64 × 64), Each time-point included 18 contiguous slices covering whole cerebrum. The EPI scan lasted from 5 min to 6 min 27 s. Finally, a 3D spoiled GRE scan was performed (TR = 70 ms, TE = 4.2 ms, flip angle = 20, slice thickness = 1.5 mm, slice gap = 0 mm, FOV = 240 mm, matrix = 192 × 256).

2.3. Data analysis

FMRI data preprocessing was performed with SPM2 (http://www.fil.ion.ucl.ac.uk/spm). The first three volumes were discarded. Then, images were corrected for slice-timing and realigned to the first image for rigid-body head movement correction (patient data with movement greater than 3 mm was discarded). Afterwards, the functional images were normalized into standard stereotaxic anatomical Montreal Neurological Institute (MNI) space. The normalized volumes were resampled to a voxel size of 3 mm × 3 mm × 3 mm. As a final step, EPI images were spatially smoothed using isotropic Gaussian filter (5-mm FWHM).

Before functional connectivity analysis, all image data was simply filtered by a phase-insensitive bandpass filter (pass band 0.01–0.08 Hz) to reduce the effect of low frequency drift and high frequency physiological noise, and voxel intensities were scaled by dividing the value at each time point by the mean value of the whole brain image at that time point to minimizing the effect of global drift. Then, we selected the PCC template as the region of interest (ROI), which consist of Brodmann areas 29, 30, 23, and 31 using the WFU-PickAtlas software [26,27]. Finally, in order to perform the ROI-based correlation analysis, the mean PCC signal intensity was calculated by averaging the time series of all voxels in the selected ROI. The resulting time course was used to perform Pearson linear correlation analysis with all voxels of the brain data, and the mask images were acquired with a threshold of correlation coefficients [16,30]. A Fisher *z*-transform was applied to normalize the correlation coefficients [9,16]. The individual *z* scores were entered into SPM2 for random-effects one-sample *t*-test to determine brain regions with significant connectivity to the PCC within each group. These individual scores were also entered into SPM2 for random-effects analyses and two-sample *t* tests to identify regions with significant differences in connectivity to the PCC between groups. Regions with statistical significance were masked on MNI brain templates.

Table 2
Significant connectivity difference between-group contrasts with their locations

Regions	MNI coordinates			Peak *T* score	No. of cluster voxels
	x	*y*	*z*		
Control > mild AD					
VMPFC	6	55	47	3.57	19
L visual cortex	−27	−99	−14	4.24	81
R visual cortex	35	−95	−14	3.22	14
R DLPFC	24	−30	66	3.12	38
	38	−21	33	3.04	3
	48	−12	66	3.00	17
L ITC	54	−38	−25	3.81	55
R ITC	−58	−16	−27	3.30	7
L hippocampus	−21	−27	−9	2.83	6
R thalamus	15	−18	15	3.80	17
Precuneus	−22	−70	60	2.66	7
Mild AD > control					
MPFC	−13	54	23	2.96	11
L PMC	−45	33	48	4.84	136
L DLPFC	−45	24	18	4.09	22
	−51	3	15	3.62	18
R DLPFC	57	42	24	3.35	5
R OFC	12	57	−15	3.72	11
L ITC	−33	−9	−36	3.66	14

MPFC: medial prefrontal cortex; DLPFC: dorsal lateral prefrontal cortex; ITC: inferior temporal cortex; PMC: primary motor cortex; OFC: orbital frontal cortex; R: right; L: left ($p < 0.01$, corrected with FDR; extent threshold = 5 voxel).

3. Results

3.1. Demography and neuropsychological test

Demographic characteristics and neuropsychological scores were shown in Table 1. No significant differences in gender, age and educational level were noted between both experimental groups. But MMSE was significantly different between groups using the *F*-test (two-way ANOVA, $F = 89.3$, $p < 0.0001$).

3.2. PCC connectivity: within-group analyses

Data from two patients were eliminated from the subject group because of excessive head movement. Within-group analysis was performed using SPM2, and the statistical threshold was set at the level of corrected with false discovery rate (FDR) *p* value <0.01 and extent threshold = 5 voxels. Regions with connectivity to the PCC in each of groups were obtained, and these two intergroup maps appeared to be similar during visual inspection (Fig. 1). Primary regions involved in the network in control group include the ventral MPFC, the bilateral hippocampus, ITC, pulvinars, visual cortices, cuneus/precuneus and IPC. These regions coincide with regions underlying the default mode network [18–20].

3.3. PCC connectivity: between-group analyses

Between-group analyses were performed using an SPM2 two-sample *t*-test, with the statistic threshold of corrected with FDR $p < 0.01$ and extent threshold = 5 voxels. The between-group difference in PCC connectivity was obtained. We compared control group with the AD group, and this contrast showed a pattern of reduced interaction with PCC in AD groups or areas of disconnectivity. Decreased connectivity was detected in the regions of the bilateral visual cortex, the ITC, the posterior orbital frontal cortex (POFC), ventral MPFC and precuneus. In particular, the left hippocampus, right thalamus, right dorsal–lateral prefrontal cortex (DLPFC) showed left/right asymmetry (details see Table 2, Fig. 2). Conversely, we also compared the AD group with the control group, and this comparison showed a pattern of higher interaction with PCC in AD brain groups or increasing connectivity. Significant coactivation was found in bilateral DLPFC, left basal ganglia, left ITC, bilateral posterior orbital prefrontal cortex, MPFC in mild AD brain with conspicuous leftward asymmetry, especially in the left primary motor cortex (details see Table 2, Fig. 3).

4. Discussion

In the present study, we assessed FC in mild AD brain by studying the spatialtemporal correlation without a focal task. It has been established that the spatial and temporal properties of synchronous LFFs have a neuronal foundation [31]. Data from animal literature has revealed that there are prominent connectivities between PCC and medial temporal lobe structures [32], such as the hippocampus and the entorhinal cortex, which are among the earliest regions affected by AD pathology [28,29], which in turn could affect the synchrony of the LFF in the medial temporal lobe. Thus, impaired medial temporal lobe connectivity can be reflected readily through PCC connectivity, although PCC is not affected by NFT of AD pathology at the early stage [33]. Recent diffusion tensor MR imaging findings in preclinical or early AD patients have suggested impairments to ultrastructural integrity of white matter tracts in the hippocampus and decreased fiber connections between the hippocampus and the PCC [34,35].

The mechanism of resting-state brain networks still remains unclear, although a few resting fMRI investigations have been performed in AD. These investigations suggest that in the early stage of AD, connectivities between PCC and hippocampus, anterior cingulate cortex, MPFC and precuneus are disrupted [15–17].

PCC is a region of multiple cytoarchitectonics with multiple connection pathways which altered in our finding. We find that MPFC, left hippocampus and right DLPFC appear to have disrupted connectivity to PCC (Fig. 2). These structures as well as PCC are among networks constructing episodic memorial functional–anatomical systems [18,19,36], and are usually activated or deactivated during a series of neuro-imaging studies related to memory process [12,18,19,21,22]. Unlike some studies showing connectivity between PCC and right or both hippocampus [16,17], our study showed that the lateralized disconnection between PCC and left hippocampus occurs during early degeneration stage, which agrees with the findings that hypometabolism and atrophy occur in the predominant left hemisphere rather than the right at the early AD stage [37,38]. The finding of PCC-left hippocampus connectivity is also consistent with results found by Greicius et al. [15]. Lateralization is likely due to the typical predominant of the left hemisphere, which is more vulnerable than the right in AD. In addition to memory impairment, various types of cognitive decline are also associated with MPFC deficit because MPFC plays an important role in the monitoring of behavioral acts, attention shift, self reflection, emotion and social cognition [39,40].

We observed that the regions of the bilateral primary visual cortices, ITC, precuneus and right thalamus showed decreased connectivity to the PCC. These regions are implicated in the dorsal and ventral visual processing pathways, and many high-level visual functions are impaired in early AD [41,42]. Consistent with previous studies, our findings demonstrate that damaged functional linkage within both visual pathways in resting-state may contribute to impairment of higher visual functions in early AD. There are discrepancies in the case of bilateral thalamus function, as the right thalamus is more involved in visual-spatial function than its counterpart which is more involved in language function [43]. The appearance of right thalamus-PCC dissociation could indicate that visual-spatial damage is an early clinical manifestation in AD patients. There were no similar results in previous studies regard-

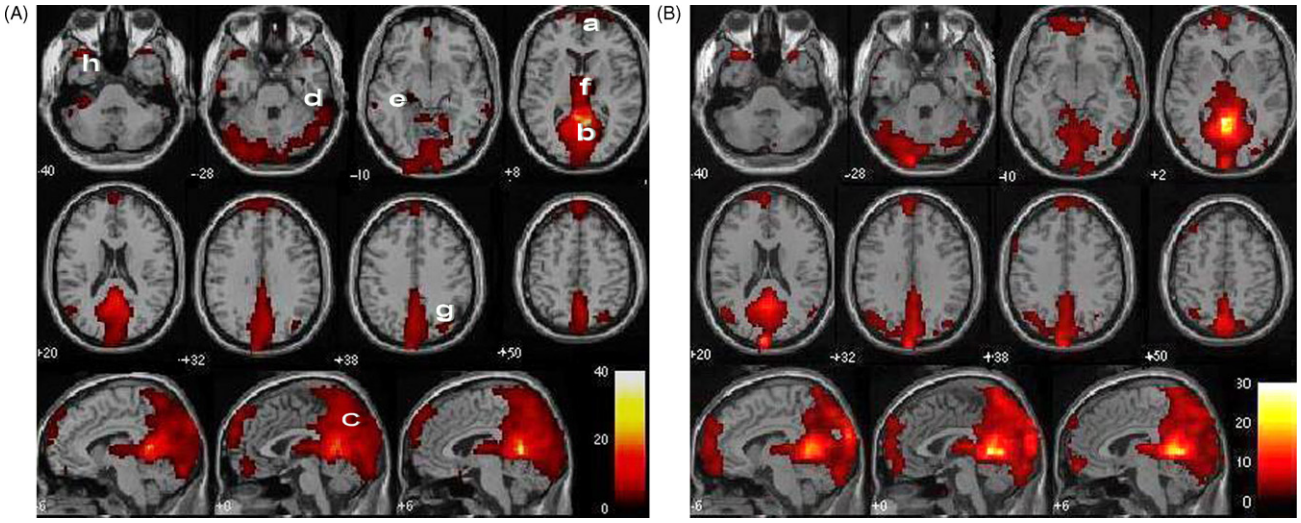

Fig. 1. Intragroup maps of connectivity to PCC of resting-state networks. (A) Control group; (B) mild AD group. Significant connectivity regions are superimposed on SPM 152T1 template ($p < 0.01$, corrected with FDR; extent threshold = 5 voxel). (a) Ventral MPFC; (b) PCC; (c) precuneus/cuneus; (d) ITC; (e) hippocampus; (f) thalamus; (g) IPC; (h) temporal pole. Left is left. The color scale represents t values.

ing the disrupted right thalamus-PCC connection [15–17]. We also observed a disruption in the connection between the POFC and the PCC (Fig. 2). The POFC is a part of the basal forebrain where AD pathology is initiated, and dominates olfactory perception function. Loss of olfactory perception is one of the preclinical symptoms of AD [44,45]. Therefore, we reason that a disruption of the functional connection between PCC and POFC may contribute to impairment of olfactory sensation in early AD.

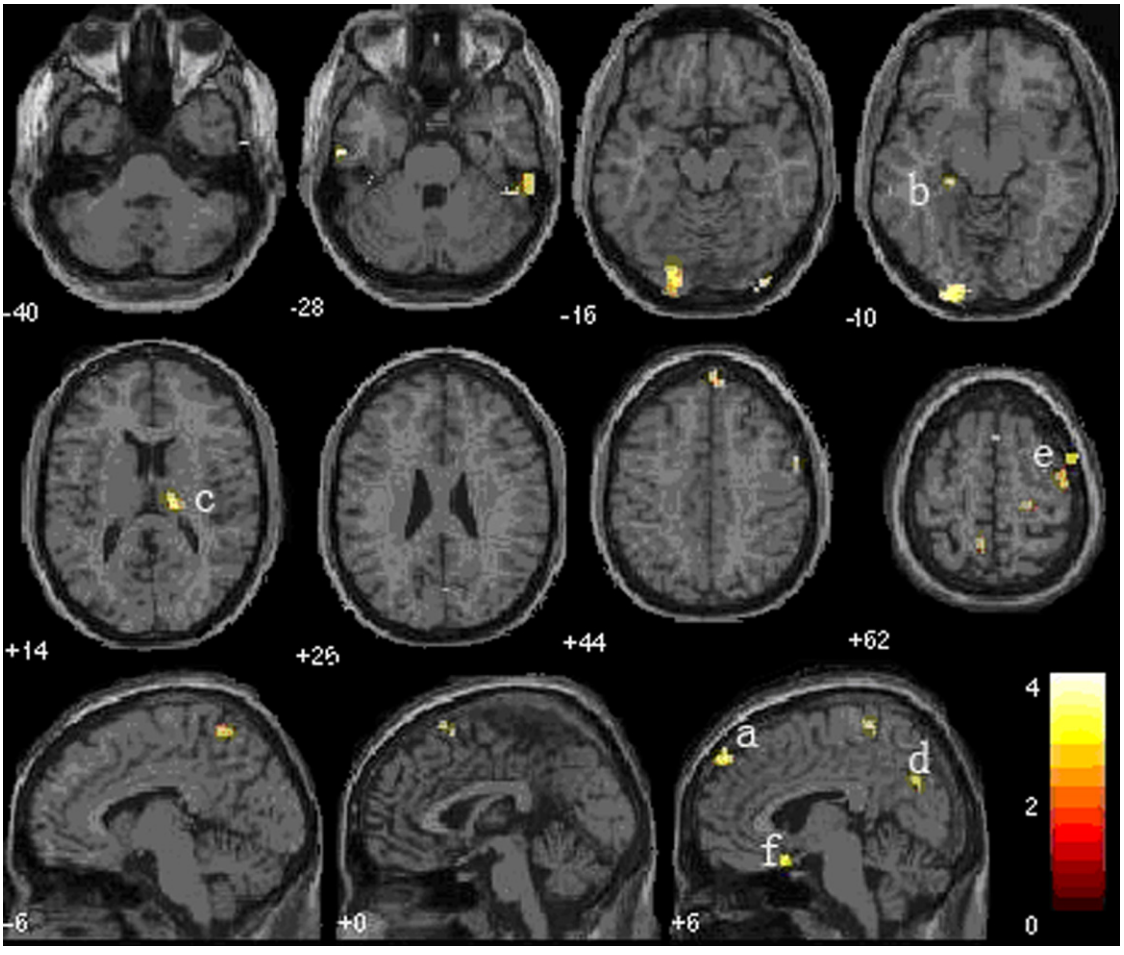

Fig. 2. Location of regions showing decreased connectivity in AD group. Regions are superimposed on SPM 152 T1WI template ($p < 0.01$, corrected with FDR; extent threshold = 5 voxel). (a) MPFC; (b) hippocampus; (c) thalamus; (d) precuneus; (e) right DLPFC; (f) POFC. Left is left. The color scale represents t values.

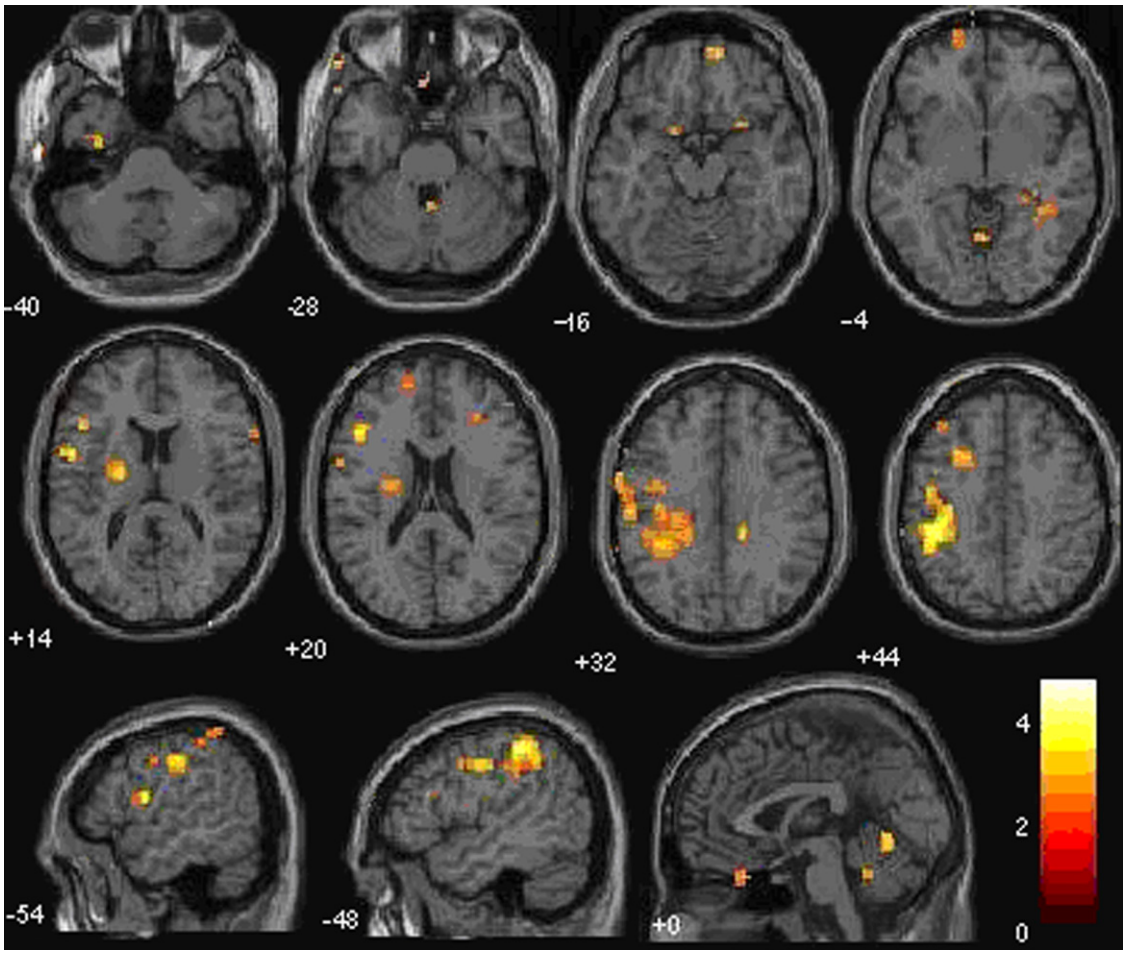

Fig. 3. Location of regions showing increased connectivity in AD group. Regions are superimposed on SPM 152 T1WI template ($p < 0.01$, corrected with FDR; extent threshold = 5 voxel). Left is left. The color scale represents t values. Prominent left asymmetry of increased connectivity can be seen particularly at areas of left motor related cortices, left dorsal lateral prefrontal cortex and left basal ganglia.

These results support our hypothesis that enhanced connectivity to PCC occurs mostly in the asymmetric regions of left ITC, left lateral prefrontal cortex extending into left primary motor cortex. The enhanced interaction with the PCC may be regarded as a compensation for the loss of disrupted FC. Neuro-imaging studies have shown that AD patients showed additional left DLPFC activation in semantic memory tasks, and increased functional connectivity within the prefrontal regions [16,46,47]. In our study, the result of increased PCC functional connections primarily in the left frontal–parietal cortices is also consistent with findings in AD pathological marker infestation staging [28,29], which show that medial temporal lobes are vulnerable early, whereas the frontal cortex, sensory and motor cortices incur encroachments later. These later impaired regions may be recruited preferentially to compensate for the early incurred damage. An alternative explanation for the increased connections is the loss of inhibitory influence. An intriguing and unpredicted region showing increased functional connectivity is the left basal ganglia. It has been observed by Haber et al. [48] in monkey using in vivo neuronal projection tracers that there are parallel reciprocation pathways between the MPFC and the globus pallidus, but that the prefrontal cortex plays an inhibitive role on basal ganglia [49]. Therefore, it is possible that decreased activity in the MPFC and the PCC may have less repression on the basal ganglia and therefore contribute to its increased activation.

There were a few limitations in our methods. The defects of temporal correlation method with a seeding region have been previously discussed [50]. When we extracted LFF with a band of 0.01–0.08 Hz, the cardiac and respiratory fluctuation effects were not completely eliminated from the LFFs [9,25,50]. These aliasing effects might have reduced the specificity of the connectivity effects. However, it must be noted that previous results from Cordes et al. [8] indicated that physiological noise sources, such as respiratory or cardiac pulsations, had little effect on the cross-correlation coefficients in defining functional connectivity maps. We arbitrarily imposed a PCC template on all subject brains after normalization, disregarding differences between individuals in PCC atrophy volume. It is possible that atrophy in PCC may influence functional connectivity, but should be minor. He et al. [14] revealed that a decrease in regional LLF coherence was partly associated with PCC volume atrophy. Whereas there is evidence in PET findings that regional glucose metabolic abnormalities were not attributed to atrophy in Alzheimer's disease [51].

In summary, bidirectional changes of FC in the current study bring insight to the links between different AD brain regions. Defects in PCC-related resting networks in the early AD stage contained both disruptions and compensations of functional connectivity. The disrupted PCC functional connectivity may be associated with a series of neuronal impairments in AD patients. In the future experimentation, we hope to investigate the correlations between connectivity strength and neuropsychological test score. We are also interested in following the changes in functional connectivity through the progression of AD.

Acknowledgments

We make a grateful acknowledgement for the innominate reviewers. This work was supported by the Scientific Research Foundation of Graduate School of Southeast University; we are grateful to staff at geropsychiatry clinic department, Nanjing Brain Hospital for providing and caring for study patients. We are grateful to Dr. Min Wu for his help in MR data collection.

This study was sponsored by "973 project of No. 2007CD512303". We thank Ms. Rui Dong, from Duke University, class of 2011 for her help for editing on this manuscript.

References

[1] Delbeuck X, Van der Linden M, Collette F. Alzheimer's disease as a disconnection syndrome? Neuropsychol Rev 2003;13:79–92 [PMID: 12887040].
[2] Wevers A, Burghaus L, Moser N, Witter B, Steinlein OK, Schütz U, et al. Expression of nicotinic acetylcholine receptors in Alzheimer's disease: postmortem investigations and experimental approaches. Behav Brain Res 2000;113:207–15 [PMID: 10942047].
[3] Lau CG, Zukin RS. NMDA receptor trafficking in synaptic plasticity and neuropsychiatric disorders. Nat Rev Neurosci 2007;8:413–26 [PMID:17514195].
[4] Adalbert R, Gilley J, Coleman MP. Abeta, tau and ApoE4 in Alzheimer's disease: the axonal connection. Trends Mol Med 2007;13:135–42 [PMID: 17344096].
[5] Berg L, McKeel Jr DW, Mille JP, Storandt M, Rubin EH, Morris JC, et al. Clinicopathologic studies in cognitively healthy aging and Alzheimer's disease: relation of histologic markers to dementia severity, age, sex, and apolipoprotein E genotype. Arch Neurol 1998;55:326–35 [PMID: 9520006].
[6] Tiraboschi P, Hansen LA, Thal LJ, Corey-Bloom J. The importance of neuritic plaques and tangles to the development and evolution of AD. Neurology 2004;62:1984–9 [PMID: 15184601].
[7] van de Ven VG, Formisano E, Prvulovic D, Roeder CH, Linden DE. Functional connectivity as revealed by spatial independent component analysis of fMRI measurements during rest. Hum Brain Mapp 2004;22:165–78 [PMID: 15195284].
[8] Cordes D, Haughton VM, Arfanakis K, Carew JD, Turski PA, Moritz CH, et al. Frequencies contributing to functional connectivity in the cerebral cortex in "Resting-state" data. Am J Neuroradiol 2001;22:1326–33 [PMID: 11498421].
[9] Biswal B, Yetkin FZ, Haughton VM, Hyde JS. Functional connectivity in the motor cortex of resting human brain using echo-planar MRI. Magn Reson Med 1995;34(4):537–41 [PMID: 8524021].
[10] Lowe MJ, Mock BJ, Sorenson JA. Functional connectivity in single and multislice echoplanar imaging using resting-state fluctuations. NeuroImage 1998;7(2):119–32 [PMID: 9558644].
[11] Hampson M, Peterson BS, Skudlarski P, Gatenby JC, Gore JC. Detection of functional connectivity using temporal correlations in MR images. Hum Brain Mapp 2002;15:247–62 [PMID: 11835612].
[12] Celone KA, Calhoun VD, Dickerson BC, Atri A, Chua EF, Miller SL, et al. Alterations in memory networks in mild cognitive impairment and Alzheimer's disease: an independent component analysis. J Neurosci 2006;26:10222–31 [PMID: 17021177].
[13] Li SJ, Li Z, Wu G, Zhang MJ, Franczak M, Antuono PG. Alzheimer disease: evaluation of a functional MR imaging index as a marker. Radiology 2002;225:253–9 [PMID: 12355013].
[14] He Y, Wang L, Zang Y, Tian L, Zhang X, Li K, et al. Regional coherence changes in the early stages of Alzheimer's disease: a combined structural and resting-state functional MRI study. NeuroImage 2007;35:488–500 [PMID: 17254803].
[15] Greicius MD, Srivastava G, Reiss AL, Menon V. Default-mode network activity distinguishes Alzheimer's disease from healthy aging: evidence from functional MRI. PNAS 2004;101:4637–42 [PMID: 15070770].
[16] Wang L, Zang Y, He Y, Liang M, Zhang X, Tian L, et al. Changes in hippocampal connectivity in the early stages of Alzheimer's disease: evidence from resting state fMRI. NeuroImage 2006;31:496–550 [PMID: 16473024].
[17] Sorg C, Ried V, Muhlau M, Calhoun VD, Eichele T, Läer L, et al. Selective changes of resting-state networks in individuals at risk for Alzheimer's disease. PNAS 2007;104:18760–5 [PMID: 18003904].
[18] Gusnard DA, Raichle ME. Searching for a baseline: functional imaging and the resting human brain. Nat Rev Neurosci 2001;2:685–92 [PMID: 11584306].
[19] Greicius MD, Krasnow B, Reiss AL, Menon V. Functional connectivity in the resting brain: a network analysis of the default mode hypothesis. PNAS 2003;100:253–8 [PMID: 12506194].
[20] De Luca M, Beckmann CF, De Stefano N, Matthews PM, Smith SM. fMRI resting state networks define distinct modes of long-distance interactions in the human brain. NeuroImage 2006;29:1359–67 [PMID: 16260155].
[21] Ries ML, Schmitz TW, Kawahara TN, Torgerson BM, Trivedi MA, Johnson SC. Task-dependent posterior cingulate activation in mild cognitive impairment. NeuroImage 2006;29:485–92 [PMID: 16102979].
[22] Whishaw IQ, Wallace DG. On the origins of autobiographical memory. Behav Brain Res 2003;138:113–9 [PMID: 12527442].
[23] Chetelat G, Desgranges B, de la Sayette V, Viader F, Eustache F, Baron JC. Mild cognitive impairment: can FDG-PET predict who is to rapidly convert to Alzheimer's disease? Neurology 2003;60:1374–7.
[24] Hirao K, Ohnishi T, Hirata Y, Yamashita F, Mori T, Moriguchi Y, et al. The prediction of rapid conversion to Alzheimer's disease in mild cognitive impairment using regional cerebral blood flow SPECT. Neuroimage 2005;28:1014–21 [PMID: 16129627].
[25] Cordes D, Haughton VM, Arfanakis K, Wendt GJ, Turski PA, Moritz CH, et al. Mapping functionally related regions of brain with functional connectivity MR imaging. Am J Neuroradiol 2000;21:1636–44 [PMID: 11039342].
[26] Maldjian JA, Laurienti PJ, Burdette JB, Kraft RA. An automated method for neuroanatomic and cytoarchitectonic atlas-based interrogation of fMRI data sets. NeuroImage 2003;19:1233–9 [PMID: 12880848].
[27] Maldjian JA, Laurienti PJ, Burdette JH. Precentral gyrus discrepancy in electronic versions of the Talairach atlas. Neuroimage 2004;21:450–5 [PMID: 14741682].
[28] Braak H, Braak E. Neuropathological staging of Alzheimer related changes. Acta Neuropathol 1991;82:239–59.
[29] Braak H, Braak E. Staging of Alzheimer-related cortical destruction. Int Psychogeriatr 1997;9(Suppl. 1):257–61, discussion 269–272 [PMID: 9447446].
[30] Wang S, Zhang Z, Lu G, Luo L. Localization of brain activity by temporal anti-correlation with the posterior cingulate cortex. Conf Proc IEEE Eng Med Biol Soc 2007:5227–30 [PMID: 18003186].
[31] McCormick DA. Spontaneous activity: signal or noise? Science 1999;285(5427):541–3 [PMID: 10447487].
[32] Lavenex P, Suzuki WA, Amaral DG. Perirhinal and parahippocampal cortices of the macaque monkey: projections to the neocortex. J Comp Neurol 2002;447:394–420 [PMID: 11992524].
[33] Delacourte A, David JP, Sergeant N, Buee L, Wattez A, Vermersch P, et al. The biochemical pathway of neurofibrillary degeneration in aging and Alzheimer's disease. Neurology 1999;52:1158–65.
[34] Fellgiebel A, Wille P, Müller MJ, Winterer G, Scheurich A, Vucurevic G, et al. Ultrastructural hippocampal and white matter alterations in mild cognitive impairment: a diffusion tensor imaging study. Dement Geriatr Cogn Disord 2004;18:101–8 [PMID: 15087585].
[35] Zhou Y, Dougherty Jr JH, Hubner KF, Bai B, Cannon RL, Hutson RK. Abnormal connectivity in the posterior cingulate and hippocampus in early Alzheimer's disease and mild cognitive impairment. Alzheimers Dement 2008;4:265–70 [PMID: 18631977].
[36] Budson AE, Price BH. Memory dysfunction. N Engl J Med 2005;352:692–9 [PMID: 15716563].
[37] Loewenstein DA, Barker WW, Chang JY, Apicella A, Yoshii F, Kothari P, et al. Predominant left hemisphere metabolic dysfunction in dementia. Arch Neurol 1989;46:146–52 [PMID: 2783845].
[38] Janke AL, de Zubicaray G, Rose SE, Griffin M, Chalk JB, Galloway GJ. 4D deformation modeling of cortical disease progression in Alzheimer's dementia. Magn Reson Med 2001;46:661–6.
[39] Iacoboni M, Lieberman MD, Knowlton BJ, Molnar-Szakacs I, Moritz M, Throop CJ, et al. Watching social interactions produces dorsomedial prefrontal and medial parietal BOLD fMRI signal increases compared to a resting baseline. NeuroImage 2004;21:1167–73 [PMID: 15006683].
[40] Chee MW, Tan JC. Inter-relationships between attention, activation, fMR adaptation and long-term memory. Neuroimage 2007;37:1487–95 [PMID: 17689983].
[41] Prvulovic D, Hubl D, Sack AT, Melillo L, Maurer K, Frölich L, et al. Functional imaging of visuospatial processing in Alzheimer's disease. NeuroImage 2002;17:1403–14 [PMID: 12414280].
[42] Tales A, Butler S. Visual mismatch negativity highlights abnormal preattentive visual processing in Alzheimer's disease. Neuroreport 2006;17:887–90 [PMID: 16738482].
[43] Schmahmann JD. Vascular syndromes of the thalamus. Stroke 2003; 34:2264–78 [PMID: 12933968].
[44] Wang QS, Tian L, Huang YL, Qin S, He LQ, Zhou JN. Olfactory identification and apolipoprotein E epsilon 4 allele in mild cognitive impairment. Brain Res 2002;951:77–81 [PMID: 12231459].
[45] Peters JM, Hummel T, Kratzsch T, Lotsch J, Skarke C, Frolich L. Olfactory function in mild cognitive impairment and Alzheimer's disease: an investigation using psychophysical and electrophysiological techniques. Am J Psychiatry 2003;160:1995–2002 [PMID: 14594747].
[46] Horwitz B, McIntosh AR, Haxby JV, Furey M, Salerno JA, Schapiro MB, et al. Network analysis of PET-mapped visual pathways in Alzheimer type dementia. Neuroreport 1995;27:2287–92.
[47] Saykin AJ, Flashman LA, Frutiger SA, Johnson SC, Mamourian AC, Moritz CH, et al. Neuroanatomic substrates of semantic memory impairment in Alzheimer's disease: patterns of functional MRI activation. J Int Neuropsychol Soc 1999;5:377–92.
[48] Haber SN, Kunishio K, Mizobuchi M, Lynd-Balta E. The orbital and medial prefrontal circuit through the primate basal ganglia. J Neurosci 1995;75:4851–67 [PMID:7623116].
[49] de Jong BM, Paans AM. Medial versus lateral prefrontal dissociation in movement selection and inhibitory control. Brain Res 2007;1132:139–47 [PMID: 17173869].
[50] Thirion B, Dodel S, Poline JB. Detection of signal synchronizations in resting-state fMRI datasets. NeuroImage 2006;29:321–7 [PMID:16129624].
[51] Ibanez V, Pietrini P, Alexander GE, Furey ML, Teichberg D, Rajapakse, et al. Regional glucose metabolic abnormalities are not the result of atrophy in Alzheimer's disease. Neurology 1998;50:1585–93 [PMID: 9633698].